

Weak Coupling Phases of the Attractive $t - t'$ Hubbard Model at the Van Hove Filling

J. V. Alvarez¹ and J. González²

¹*Departamento de Matemáticas. Universidad Carlos III. Butarque 15. Leganés. 28913 Madrid. Spain.*

²*Instituto de Estructura de la Materia. Consejo Superior de Investigaciones Científicas. Serrano 123, 28006 Madrid. Spain.*
(November 19, 2018)

We apply a wilsonian renormalization group approach to the continuum limit of the attractive $t - t'$ Hubbard model, taken when the Fermi level is at the Van Hove singularity of the density of states. The model has well-defined scaling properties and the effective couplings display an unbounded flow in the infrared. We determine the leading instabilities by computing the different response functions up to $t' = 0.5t$. The phase diagram shows a large boundary between superconducting and charge-density-wave phases, that merge in a triple point with a phase separation instability. The latter is realized down to very low coupling constant, as the Fermi sea degenerates towards a pair of straight lines near $t' = 0.5t$.

71.27.+a, 74.20.Mn

During recent years there has been important progress in understanding the properties of quantum electron liquids in dimension $D < 3$. One of the most fruitful approaches in this respect springs from the use of renormalization group (RG) methods, in which the different liquids are characterized by several fixed-points controlling the low-energy properties. The Landau theory of the Fermi liquid in dimension $D > 1$ can be taken as a paradigm of the success of this program. It has been shown that, at least in the continuum limit, a system with isotropic Fermi surface and regular interaction is susceptible of developing a fixed-point in which the interaction remains stable in the infrared¹. This example is of particular significance since there are systems that do not lie in the perturbative regime, and yet we know that their description in terms of the effective Fermi liquid theory is correct, as its predictions apply fairly well.

The question of whether different critical points may arise at dimension $D = 2$ is now a subject of debate²⁻⁵. The interest has risen in parallel to the failure of a global theoretical understanding of the high- T_c superconductivity of the cuprates. The two-dimensional Hubbard model has been proposed long time ago as the correct starting point to study the electronic correlations inside the copper oxide planes⁶, and several authors have also proposed recently that it should have a quantum critical point separating antiferromagnetic and d-wave superconducting phases⁷. However, the elucidation of the existence of such critical point is quite difficult, specially in the strong coupling regime, since the presence of the strong correlations do not make obvious even the determination of the continuum limit of the model. Actually, apart from the above mentioned case of regular Fermi surface, in general it is not possible to find by simple inspection of the microscopic hamiltonian a set of scaling operators that behave properly under RG transformations. This is particularly true in the case of the Hubbard model at half-filling.

The above considerations stress the interest of identifying microscopic models with correct scaling properties from the RG point of view. The $t - t'$ Hubbard model filled up to the level of the Van Hove singularity provides such an example. The determination of the scaling properties and low-energy phases for repulsive interaction has been accomplished in Ref. 8 (see also Ref. 9). We are interested now in the case of the $t - t'$ Hubbard model at negative U , which highlights some important properties of the electron interactions near a Van Hove singularity.

We briefly review the way in which the low-energy limit is taken in the model, and how in this case a set of scaling operators can be read at once from the hamiltonian¹⁰. High-energy and low-energy electron modes are separated by an energy cutoff E_c , that is sent progressively towards the Fermi line as high-energy modes are integrated out in the RG process. When the Fermi level is at the Van Hove singularity, as shown in Fig. 1, most part of the low-energy states close to the Fermi line are concentrated around the saddle points at $(\pi, 0)$ and $(0, \pi)$, as these features are at the origin of the divergent density of states. Therefore, in building up the low-energy effective theory we may focus on two patches around the respective saddle points A and B , where the dispersion relation can be approximated by

$$\varepsilon_{A,B}(\mathbf{k}) \approx \mp(t \mp 2t')k_x^2 a^2 \pm (t \pm 2t')k_y^2 a^2 \quad (1)$$

a being the lattice constant. In the continuum limit the rest of modes are irrelevant, from the RG point of view. In fact, the effective action for the low-energy modes restricted to the region $|\varepsilon_\alpha(\mathbf{k})| \leq E_c$ is given by

$$S = \int d\omega d^2k \sum_{\alpha,\sigma} (\omega a_{\alpha,\sigma}^+(\mathbf{k}, \omega) a_{\alpha,\sigma}(\mathbf{k}, \omega) - \varepsilon_\alpha(\mathbf{k}) a_{\alpha,\sigma}^+(\mathbf{k}, \omega) a_{\alpha,\sigma}(\mathbf{k}, \omega)) \\ - U \int d\omega d^2k \rho_\uparrow(\mathbf{k}, \omega) \rho_\downarrow(-\mathbf{k}, -\omega) \quad (2)$$

where $a_{\alpha,\sigma}(a_{\alpha,\sigma}^+)$ are electron annihilation (creation) operators (α labels the Van Hove point) and $\rho_{\uparrow,\downarrow}$ are the density operators in momentum space. Under a change in the cutoff $E_c \rightarrow sE_c$, with a corresponding scaling of the momenta $\mathbf{k} \rightarrow s^{1/2}\mathbf{k}$, one can check that the effective action remains scale invariant after an appropriate scale transformation of the electron modes $a_{\alpha,\sigma} \rightarrow s^{-3/2}a_{\alpha,\sigma}$ ¹⁰. We have therefore a microscopic model with a well-defined scaling behavior, susceptible of being studied by means of RG methods.

As E_c is sent towards the Fermi level and the electron modes are labelled according to the saddle point they are attached to, the interactions may be classified in the form shown in Fig. 2. The four possible types of local interaction U_{intra} , U_{inter} , U_{back} and U_{umk} are renormalized by quantum corrections, following a conventional pattern from the quantum field theory point of view. By integrating high-energy excitations in the slices $E_c - dE_c < |\varepsilon| < E_c$, the lowest order $O(dE_c/E_c)$ corrections are given by the particle-hole diagram of Fig. 3(a). It is worthwhile to stress that, within this wilsonian RG approach, there are no more diagrams renormalizing the interaction coupling constants, since the particle-particle channel produces a contribution that is in general $\sim (dE_c)^2$. This point has been conveniently clarified in Ref. 1. It is only when the total momentum of the colliding particles equals zero that the particle-particle channel develops a contribution $\sim dE_c$, but this points at the correction of a correlation function, defined at a particular momentum value, rather than at the renormalization of a coupling constant.

As remarked in Ref. 8, the diagram in Fig. 3(a) corresponds to an *antiscreening* effect, that tends to enhance repulsive interactions. By the same reason, its effect in the present model is that of reducing the attractive interaction and cannot produce by itself any instability driving away from normal metallic behavior. The renormalized on-site interaction has the asymptotic behavior $U \sim 1/|\log E_c|$ as the high-energy cutoff is reduced. As observed in Ref. 11, however, there are effective interactions generated by quantum corrections that are not present in the original hamiltonian. These are interactions between currents with parallel spin, that appear through second order processes like that shown in Fig. 3(b). They are strongly momentum dependent, as the polarizabilities near $\mathbf{q} = 0$ and $\mathbf{q} = \mathbf{Q} \equiv (\pi, \pi)$ are given respectively by

$$\chi(\mathbf{q}, \omega = 0) = \frac{c}{2\pi^2 t} \log \left| \frac{E_c}{\varepsilon(\mathbf{q})} \right| \quad (3)$$

$$\chi'(\mathbf{q}, \omega = 0) = \frac{c'}{2\pi^2 t} \log \left| \frac{E_c}{ta^2(\mathbf{q} - \mathbf{Q})^2} \right| \quad (4)$$

where $c \equiv 1/\sqrt{1 - 4(t'/t)^2}$ and $c' \equiv \log \left[\left(1 + \sqrt{1 - 4(t'/t)^2}\right) / (2t'/t) \right]$. These interactions give rise to a potential that is actually singular at small momentum transfer. In real space this corresponds to an interaction decaying like $\sim 1/r^2$. It is not strange that this kind of interaction may arise in the renormalization of the model since, together with the purely local interaction, it corresponds to the other not irrelevant four-fermion operator that may appear in the effective action. According to the wilsonian RG approach, once these effective interactions appear they have to be considered on the same footing than the original bare interactions, since they are needed for the complete renormalization of the model.

The processes shown in Fig. 3(b) are singular at small momentum transfer and at momentum transfer $\sim \mathbf{Q} \equiv (\pi, \pi)$. Therefore we have to introduce new couplings V_{intra} , V_{inter} , V_{back} and V_{umk} for the effective potential between electrons with parallel spins, according to the classification in Fig. 2. The important point is that these new interactions are also attractive since they are due to *overscreening*, that is, to the screening of an interaction vanishing at the classical level.

The overscreening effect can be also understood within the RG framework, by solving the flow equations with the initial conditions $V_{intra}(E_c) = V_{inter}(E_c) = V_{back}(E_c) = V_{umk}(E_c) = 0$ at the upper value E_c of the cutoff. The most significant contributions to the renormalization of the couplings are given by the diagram in Fig. 3(b) at small momentum transfer, for V_{intra} and V_{inter} , and at momentum transfer \mathbf{Q} , for V_{back} and V_{umk} . In the diagram the interaction lines may stand either for the local interaction potential or for the $1/r^2$ potential. One has to realize that, under renormalization, $1/r^2$ effective interactions may also arise between currents with opposite spin, that we denote, conserving the previous notation, by $V_{\perp intra}$, $V_{\perp inter}$, $V_{\perp back}$ and $V_{\perp umk}$. The RG flow equations, that reflect the change of the couplings by integration of particle-hole processes at the high-energy cutoff E_c , are given by

$$E_c \frac{\partial}{\partial E_c} (V_{intra} \pm V_{inter}) = -\frac{1}{2\pi^2 t} c \left((U_{intra} \pm U_{inter})^2 + (V_{intra} \pm V_{inter})^2 + (V_{\perp intra} \pm V_{\perp inter})^2 \right) \quad (5)$$

$$E_c \frac{\partial}{\partial E_c} (V_{\perp intra} \pm V_{\perp inter}) = -\frac{1}{2\pi^2 t} c \left(2(U_{intra} \pm U_{inter})(V_{intra} \pm V_{inter}) + 2(V_{\perp intra} \pm V_{\perp inter})(V_{intra} \pm V_{inter}) \right) \quad (6)$$

and two more equations obtained from the former two by the replacements $c \leftrightarrow c'$, $X_{intra} \leftrightarrow X_{back}$ and $X_{inter} \leftrightarrow X_{umk}$ ($X = U, V, V_{\perp}$). Given that at the beginning of the RG process all the interactions vanish, except U_{intra} , U_{inter} , U_{back}

and U_{umk} that equal the value of the local attraction U , it is easily seen that the instabilities of the model are given by the flow of the V and V_{\perp} couplings, that become increasingly attractive at low energies.

The instabilities of the coupling constants characterize the different ground states of the system, which may be determined by studying the different response functions. These are correlators computed at particular values of the momentum, which signal the way in which symmetry breakdown takes place in the model. One may check that in the present case of attractive interaction ($U < 0$), the only correlators that may diverge at a given frequency are those for the operators $\sum_{\mathbf{k}} \left(a_{A\uparrow}^+(\mathbf{k})a_{A\downarrow}^+(-\mathbf{k}) + a_{B\uparrow}^+(\mathbf{k})a_{B\downarrow}^+(-\mathbf{k}) + h.c. \right)$, $\rho_{\uparrow}(\mathbf{Q}, \omega) + \rho_{\downarrow}(\mathbf{Q}, \omega)$ and $\rho_{\uparrow}(\mathbf{0}, \omega) + \rho_{\downarrow}(\mathbf{0}, \omega)$. Their response functions characterize, respectively, s-wave superconductivity (R_{SCs}), charge density wave (R_{CDW}) and phase separation (R_{PS}) instabilities.

We compute the response functions by exploiting again the scaling properties of the model. For this purpose we establish the dependence of the correlators on the cutoff E_c and, taking into account the scale invariance of the model (up to logarithmic renormalizations of the couplings), we introduce the dimensionless scaling variable E_c/ω to determine the dependence on the frequency ω . The starting point is the perturbative computation of each response function, that exhibits a logarithmic dependence on E_c/ω . In contrast to the RPA, we do not sum up the iteration of particle-hole bubbles, as this cannot be a reliable expansion of the correlator in a model with strong renormalization of the one-particle properties¹¹. Instead we compute the variation of the correlator under a reduction of E_c and write it down in terms of the correlator and coupling constants at the new value of the cutoff. This procedure is similar to that followed in the study of one-dimensional electron systems¹² or coupled one-dimensional chains¹³.

The scaling equations in the present case turn out to be

$$\frac{\partial R_{CDW}}{\partial E_c} = -\frac{2c'}{\pi^2 t} \frac{1}{E_c} - \frac{c'}{\pi^2 t} (V_{back} + V_{umk} + V_{\perp back} + V_{\perp umk}) \frac{1}{E_c} R_{CDW} \quad (7)$$

$$\frac{\partial R_{SCs}}{\partial E_c} = -\frac{c}{2\pi^2 t} \frac{\log(E_c/\omega)}{E_c} - \frac{c}{2\pi^2 t} (V_{\perp intra} + V_{\perp umk}) \frac{\log(E_c/\omega)}{E_c} R_{SCs} \quad (8)$$

$$\frac{\partial R_{PS}}{\partial E_c} = -\frac{2c}{\pi^2 t} \frac{1}{E_c} - \frac{c}{\pi^2 t} (V_{intra} + V_{inter} + V_{\perp intra} + V_{\perp inter}) \frac{1}{E_c} R_{PS} \quad (9)$$

The equation for R_{SCs} shows the nontrivial scaling factor $\log(E_c/\omega)$, as a consequence of the enhanced susceptibility at zero momentum in the particle-particle channel, that behaves as $\sim \log^2(E_c/\omega)$. Such factor is nothing but a reflection of the divergent density of states at the Van Hove singularity, and it does not spoil, in any event, the scaling properties of the model.

As remarked before, the natural scaling variable in the model is E_c/ω , what becomes now evident by inspection of the scaling equations (7)-(9). The fact that the renormalized coupling constants follow an unbounded flow may cast doubts in the reliability of the perturbative RG approach. The divergences that, as a consequence of it, are found in the response functions at certain values of E_c/ω provide, however, a way of discerning the competition between the different instabilities of the system. The response function having the strongest divergence as the value of ω/E_c is lowered characterizes the ground state of the system. According to this criterion, we have determined the different phases at weak U coupling and t' up to $0.5t$, where the Fermi sea degenerates into a pair of straight lines. The phase diagram is shown in Fig. 4. We recall that the charge-density-wave and superconducting ground states are degenerated in the $t' = 0$ attractive Hubbard model at half-filling^{14,15}. On the other hand, it has been shown that phase separation cannot take place in the Hubbard model on a bipartite lattice, at any value of the interaction¹⁶. The proof of this statement does not follow in our case, however, as the next-to-nearest neighbor hopping t' spoils the splitting into two sublattices.

Our results should be applicable in the weak coupling regime and to Fermi surfaces corresponding to an appreciable value of t' . This is because the main assumption of our RG approach is the possibility of taking the continuum limit, which neglects correlation effects due to a large on-site attraction U . These are important for the Hubbard model at or near half-filling. Otherwise, our approach provides the evidence in a concrete model of the proposed connection between charge-density-wave or phase separation instabilities and anisotropic superconductivity¹⁷. We have to bear in mind that, in our low-energy theory, the condensate wavefunction turns out to have the same sign near $(\pi, 0)$ and $(0, \pi)$ but it must have necessarily less strength far from the saddle points, leading to a highly anisotropic gap. Specially sensible is our prediction of phase separation at low filling and weak coupling, when the Fermi sea is degenerating towards a pair of straight lines near $t' = 0.5t$. The interplay between phase separation and anisotropic superconductivity has been also considered in the $t - J$ and U-V models¹⁸ as well as in the three-band Hubbard model¹⁹. Phase separation near a Van Hove singularity has been discussed in a model with electron-phonon interaction in Ref. 20.

With regard to real systems, the realization of a charge-density-wave in the model may bare a direct relation with the recent experimental observation of such instability in two-dimensional interfaces²¹. In those systems the atoms

at the surface are arranged in a triangular lattice, but the most important point is the present recognition that there is no significant nesting of the Fermi line accounting for the instability. The form of the dispersion relation has been evaluated in several instances, and it shows that the Fermi line is close to the saddle points at the boundary of the Brillouin Zone²².

From the theoretical point of view, one of the most remarkable features of the phase diagram in Fig. 4 is the existence of a triple point where the three different phases coalesce. The phase diagram is actually a map of the different ground states of the system. If we look at phase separation as an instability in which no symmetry breakdown takes place in a microscopic scale, opposite to what happens in the other two phases, we may conjecture that the triple point must correspond to a quantum critical point of the system. In fact, it has to be possible to crossover smoothly from the superconducting ground state to the charge-density-wave state through the phase separation region. The crossing of the two ground states is the distinctive feature of the quantum phase transition.

It is very suggestive the similarity that the phase diagram of Fig. 4 bears with that of the repulsive $t - t'$ Hubbard model at the Van Hove filling obtained with analogous RG techniques⁸. In that case there is a large boundary in the phase space between antiferromagnetic and d-wave superconducting phases, up to a point where the leading instability turns out to be ferromagnetism. The existence of these three phases has been confirmed by numerical methods. Before the RG analysis had been undertaken, quantum Monte Carlo computations had already provided a clear signature of ferromagnetism at $t' = 0.47t$ ²³. On the other hand, recent quantum Monte Carlo computations²⁴, as well as mean-field computations with effective interactions²⁵, are supporting the existence of a d-wave superconducting phase at intermediate values of t' . These evidences prove the predictability of the RG approach to the present model, and they reassure us that the phases discussed above should be susceptible of being obtained by alternative numerical methods. The question of the mentioned quantum critical point is important enough for being tested by other computational techniques. A number of points, like the nature of the strong coupling phases or the thermodynamic properties of the model, should be also investigated to that effect.

It is a pleasure to thank fruitful discussions with F. Guinea, S. Sorella and M. A. H. Vozmediano. This work has been partially supported by the CICYT Grant PB96-0875.

- ¹ R. Shankar, *Rev. Mod. Phys.* **66**, 129 (1994).
² P. W. Anderson, *Phys. Rev. Lett.* **64**, 1839 (1990); *Phys. Rev. Lett.* **65**, 2306 (1990).
³ J. Feldman, M. Salmhofer and E. Trubowitz, *J. Stat. Phys.* **84**, 1209 (1996).
⁴ K. Yokoyama and H. Fukuyama, *J. Phys. Soc. Jpn.* **66**, 529 (1997).
⁵ C. J. Halboth and W. Metzner, report cond-mat/9706143.
⁶ P. W. Anderson, *Science* **235**, 1196 (1987).
⁷ S. C. Zhang, *Science* **275**, 1089 (1997). R. B. Laughlin, report cond-mat/9709195.
⁸ J. V. Alvarez, J. González, F. Guinea and M. A. H. Vozmediano, report cond-mat/9705165, to be published in *J. Phys. Soc. Jpn.*
⁹ R. S. Markiewicz, report cond-mat/9611238, to be published in *J. Phys. Chem. Sol.*
¹⁰ J. González, F. Guinea and M. A. H. Vozmediano, *Europhys. Lett.* **34**, 711 (1996).
¹¹ J. González, F. Guinea and M. A. H. Vozmediano, *Nucl. Phys. B* **485**, 694 (1997).
¹² J. Solyom, *Adv. Phys.* **28**, 201 (1979).
¹³ L. Balents and M. P. A. Fisher, *Phys. Rev.* **53**, 12133 (1996).
¹⁴ R. Micnas, J. Ranninger and S. Robaskiewicz, *Rev. Mod. Phys.* **62**, 113 (1990).
¹⁵ The competition between charge-density-wave and superconducting instabilities has been also addressed in the context of three-dimensional systems by A. Aharony and A. Auerbach, *Phys. Rev. Lett.* **70**, 1874 (1993).
¹⁶ G. Su, *Phys. Rev. B* **54**, 8281 (1996).
¹⁷ A. Perali, C. Castellani, C. Di Castro and M. Grilli, *Phys. Rev. B* **54**, 16216 (1996).
¹⁸ E. Dagotto *et al.*, *Phys. Rev. B* **49**, 3548 (1994).
¹⁹ M. Grilli, R. Raimondi, C. Castellani, C. Di Castro and G. Kotliar, *Phys. Rev. Lett.* **67**, 259 (1993). R. Raimondi, C. Castellani, M. Grilli, Y. Bang and G. Kotliar, *Phys. Rev. B* **47**, 3331 (1993).
²⁰ R. S. Markiewicz, *J. Phys. Condens. Matter* **2**, 665 (1990).
²¹ J. M. Carpinelli, H. H. Weitering, E. W. Plummer and R. Stumpf, *Nature* **381**, 398 (1996); J. M. Carpinelli *et al.*, *Phys. Rev. Lett.* **79**, 2859 (1997).
²² G. Santoro, S. Sorella, F. Becca, S. Scandolo and E. Tosatti, report cond-mat/9802014.
²³ S. Sorella, R. Hlubina and F. Guinea, *Phys. Rev. Lett.* **78**, 1343 (1997).
²⁴ K. Kuroki and H. Aoki, report cond-mat/9710019.

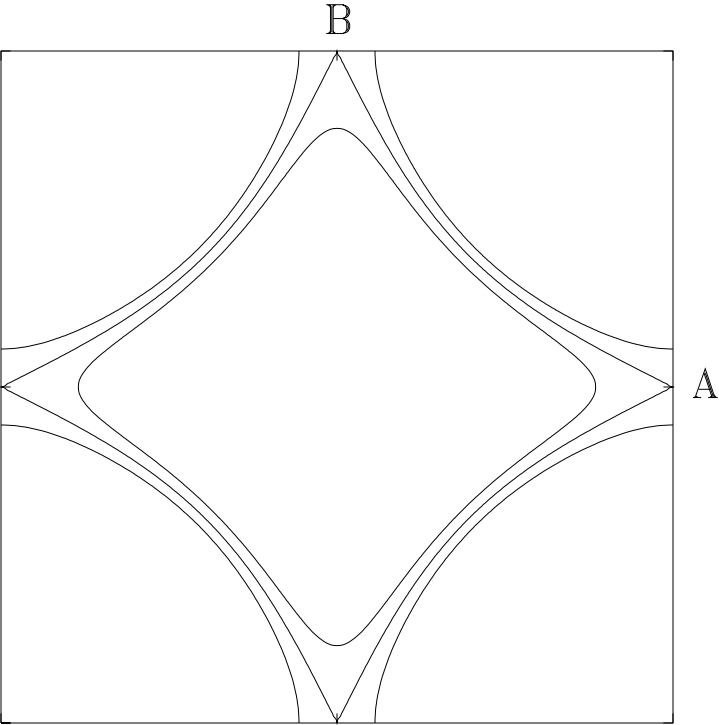
²⁵ M. Murakami and H. Fukuyama, report cond-mat/9710113.

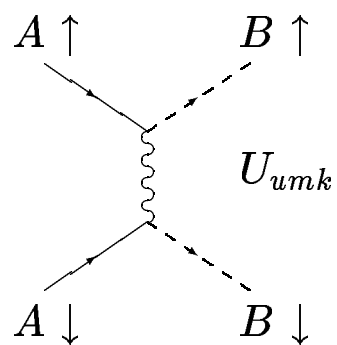
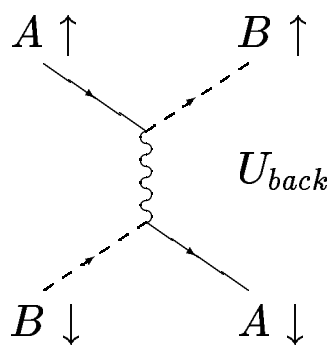
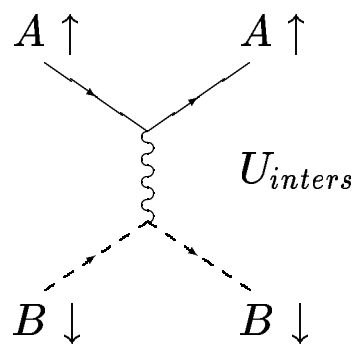
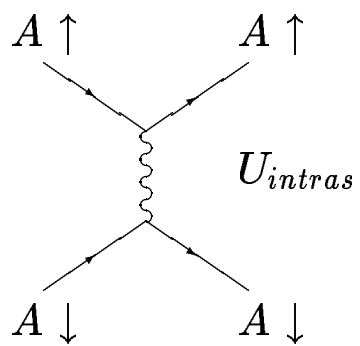
FIG. 1. Energy contour lines about the Fermi level, with the Fermi line passing by the saddle points A and B.

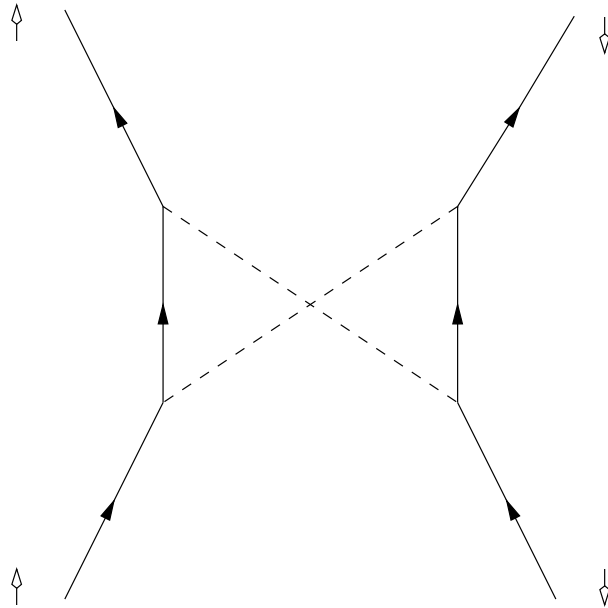
FIG. 2. Different interaction terms arising from the flavor indexes A and B.

FIG. 3. Second order diagrams renormalizing the interactions in the model, with electron lines carrying flavor index A or B appropriate to each case.

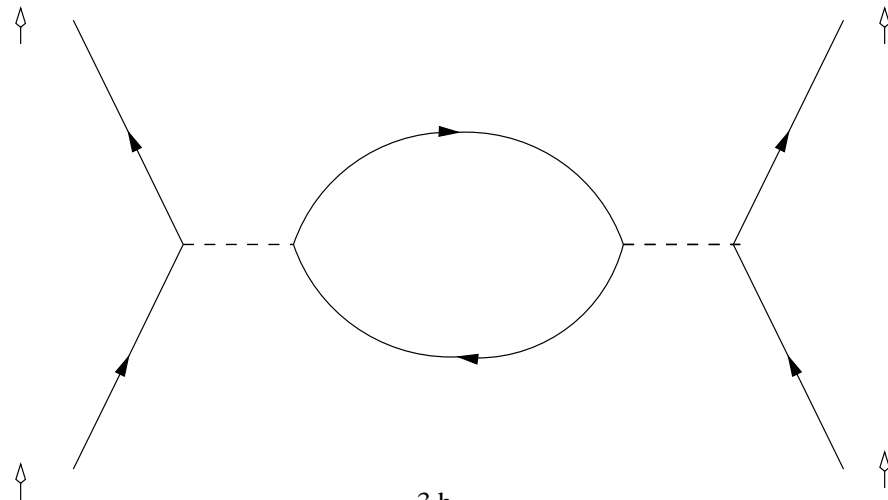
FIG. 4. Phase diagram in the (t', U) plane showing the regions of charge-density-wave (CDW), s-wave superconductivity (SC-s) and phase separation (PS) instability.







3.a



3.b

